

**ORIGINAL
RESEARCH**

J. Eggers
O. Pade
A. Rogge
S.J. Schreiber
J.M. Valdueza

Transcranial Color-Coded Sonography Successfully Visualizes All Intracranial Parts of the Internal Carotid Artery Using the Combined Transtemporal Axial and Coronal Approach

BACKGROUND AND PURPOSE: Visualization of the intracranial internal carotid artery (ICA) with transcranial color-coded sonography (TCCS) by using the transtemporal coronal plane has been described previously. Because this approach is limited to the vertical running ICA segments, we investigated the feasibility of using TCCS to visualize all intracranial ICA segments by adding the transtemporal axial approach to the coronal plane.

MATERIALS AND METHODS: Subjects with excellent transtemporal acoustic windows were examined by TCCS by using standardized axial and coronal planes. Identification rate, flow velocities, pulsatility and resistance indices, and length (as visible in color-coded power mode) were determined.

RESULTS: A total of 120 intracranial ICAs from 60 subjects were investigated. By switching between the axial and coronal insonation planes, all intracranial segments of the ICA could be investigated in 100% of subjects—with the exception of the horizontal part of the petrosal ICA, which was identified in 96.7% of subjects.

CONCLUSIONS: TCCS becomes a reliable tool in investigating all parts of the intracranial ICA by adding the transtemporal axial approach to the coronal plane.

Transcranial color-coded sonography (TCCS) is a reliable and efficient tool to gather information about the vascular state in cerebrovascular disease.¹⁻³ However, the ability of this method to visualize intracranial parts of the internal carotid artery (ICA) (Fig 1) is often neglected by most examiners. Some use the transorbital acoustic windows when they want to examine the intracranial parts of the ICA, especially the carotid siphon.⁴ This approach has many limitations, including the fact that power and insonation time have to be limited to avoid sonography-induced damage to the eye lens. Additionally, identification of different parts of the intracranial ICA by using this approach is limited and requires a highly skilled examiner.⁴ Only 2 systematic evaluations of the intracranial parts of the normal ICA and its vascular pathology by TCCS used a transtemporal approach.^{5,6} These authors did not use the axial insonation plane; they instead restricted their systematic evaluation of the ICA to the coronal axis. With this approach, only the vertical running parts of the intracranial ICA, the C1 and C5 segments, can be examined sufficiently.

The aims of this study were to show the feasibility of using a transtemporal TCCS examination to display all parts of the intracranial and distal petrosal ICA by adding the axial to the coronal approach and to determine reference values for blood-flow velocities. Therefore, the ICA was systematically studied from the horizontal part of the petrosal segment referred as the C6 to the terminal C1 segment.

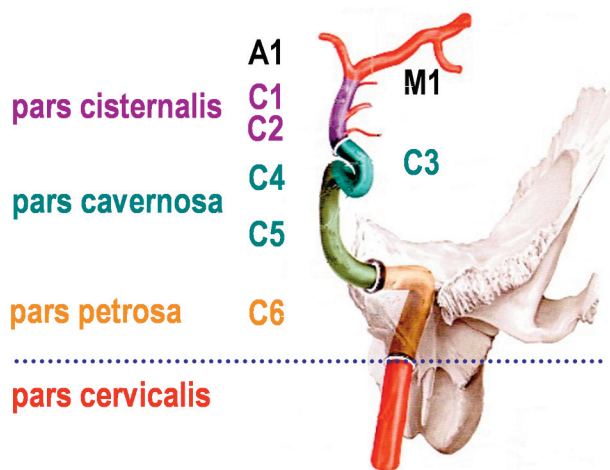


Fig 1. Sectioning of the ICA as used for sonographic examination, counting from the terminal to the proximal part to the intracranial ICA. Reprinted from Schünke et al¹⁷ with permission from Thieme Medical Publishers, Stuttgart, Germany. Note that this classification is different from the digital subtraction angiography classification, which names the cervical ICA, C1; the petrosal part, C2; and so on to the terminal ICA, C7 (Osborn¹⁸).

Materials and Methods

Subjects

Subjects were patients from our hospitals and were enrolled in the study if they had no history of cerebrovascular disease and no evidence of relevant vascular pathology, as shown by standard extracranial duplex sonography and TCCS before inclusion,¹ and if they showed a sufficient transtemporal acoustic window (fully visible M1 middle cerebral artery [MCA] and A1 anterior cerebral artery [ACA] on the examination side).² From a total of 440 patients examined at the sonography laboratory between September 2006 and March 2007, we screened 70 patients for this study; 10 of them were excluded because they showed an insufficient (completely or partially) transtemporal acoustic window. The study was approved by the local ethics committee. All subjects gave written informed consent.

Received January 15, 2009; accepted after revision February 24.

From the Department of Neurology (J.E.), Asklepios Hospital North, Hamburg, Germany; Neurological Center (O.P., A.R., J.M.V.), Segeberger Kliniken GmbH, Bad Segeberg, Germany; and Department of Neurology (S.J.S.), University Hospital Charité, Humboldt University, Berlin, Germany.

Please address correspondence to Jürgen Eggers, MD, FAHA, Neurology, Asklepios Hospital North, Tangstedter Landstr 400, 22417 Hamburg, Germany; e-mail: juergeneggers@gmx.net

DOI 10.3174/ajnr.A1602

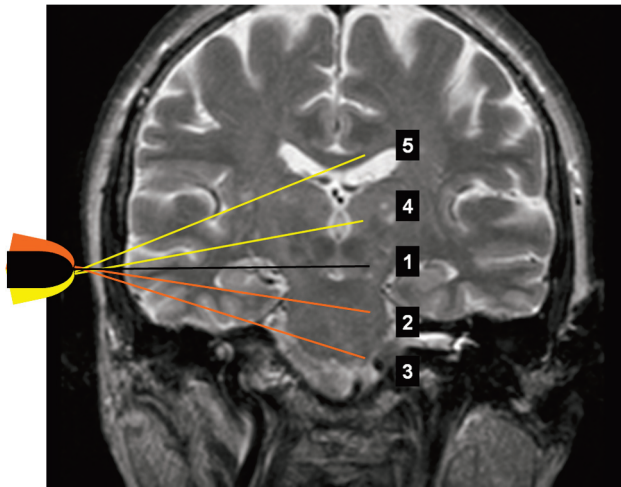


Fig 2. Planes of transtemporal axial insonation¹: midbrain,² upper pontine,³ lower pontine,⁴ thalamic,⁵ and cella media.

Sonography Protocol

TCCS measurements were performed with the patients in a supine position, by using a 2.5-MHz transcranial sector-array transducer PSM-20CT in connection with a PowerVision 6000 (SSA-370A) sonography system (Toshiba, Tokyo, Japan) transtemporally in different planes as shown in Fig 2. No sonographic contrast enhancer was used. In the color-coded power mode, red represents flow toward the transducer and blue represents flow away from the transducer. Doppler flow-velocity measurements were performed in pulsed-wave mode to determine peak-systolic and end-diastolic flow velocities. The Doppler sample volume size for flow-velocity measurement was 5.0 mm. The pulsatility index (PI) and the resistance index (RI) of the respective segments were evaluated. The length of the segment visible in color-coded mode was also measured. Angle correction was performed if the insonation angle and the visible length of the vessel were appropriate. Angle correction was considered appropriate when a straight vessel course of at least 15 mm was displayed.⁷ The visible length of the vessel segment was determined by using the color-coded power mode. MR images in standard axial and coronal planes that displayed the intracranial segments of the ICA were used to illustrate the anatomy and the correlation of the sonographic findings from the brightness- and the color-coded power modes. The examiner was free to choose gain and pulse-repetition frequencies as required to optimize the findings.

To standardize the description of the transtemporal examination, we introduced 2 additional axial planes: the upper pontine axial plane and the lower pontine plane (Fig 2).⁸ The anterior and posterior coronal planes were used for transcranial examination of the C5 and C1–2 segments. Additionally, the examiners were allowed to use oblique insonation planes when required for better visualization of the course of the vessel. However, for better reproducibility, Doppler flow-velocity measurements were performed only in axial and coronal planes.

Distal Petrosal Part (referred to as the C6 segment throughout). Using the lower pontine axial plane, the horizontal part of the petrosal segment of the ICA can be identified as a short transverse running vessel with its flow directed away from the sonographic probe. The vessel in this area is covered partly by a tiny osseous layer. The lateral rim of the petrosus bone serves as a readily identifiable anatomic landmark (Fig 3).

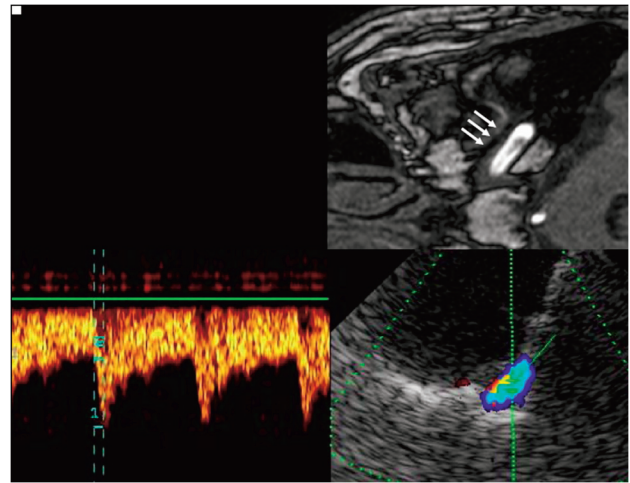


Fig 3. Assessment of the horizontal part of the C6 segment of the ICA, by using a transtemporal axial approach. Top: Time-of-flight MRA, axial source image, rotated 90° to correspond with the sonographic image. Horizontal part of the C6 segment (arrows). Bottom: TCCS, transtemporal approach, axial lower pontine plane. Right: Color-mode image demonstrates the horizontal part of the C6 segment. Left: Corresponding Doppler spectrum. Reprinted from Valdueza et al⁸ with permission from Thieme Medical Publishers, Stuttgart, Germany.

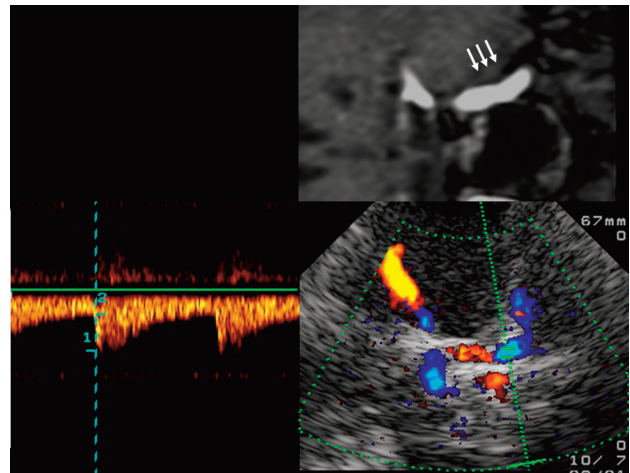


Fig 4. Assessment of the C5 segment of the ICA, by using a transtemporal coronal approach. Top: MR imaging, T1-weighted image, contrast-enhanced T1-weighted image, coronal plane, image rotated 90° to correspond with the sonographic image. Vertical part of the C5 segment (arrows). Bottom: TCCS, transtemporal approach, coronal plane. Right: Color-mode image demonstrating the C5 segment. Left: Corresponding Doppler spectrum. Reprinted from Valdueza et al⁸ with permission from Thieme Medical Publishers, Stuttgart, Germany.

To examine the C5 segment, we rotated the sonography probe 90° to the posterior coronal plane. This segment is directed toward the siphon component of the intracranial ICA. Because the insonation angle is close to 90°, the sonography transducer may detect different flow directions (toward or away from it) within the course of this segment. Blood-flow measurements in this part of the ICA do not make sense because of the unfavorable insonation angle. Therefore, we did not study the flow velocity of this segment (Fig 4).

The C3 and C4 Segments Form the Carotid Siphon (along with the C2 segment). To examine this segment, we rotated the sonography probe again 90° to the axial upper pontine plane. The course of the carotid siphon depends, along with other factors, on the age of the patient, ranging from a C-shape to omegalike and tortuous shapes.⁹

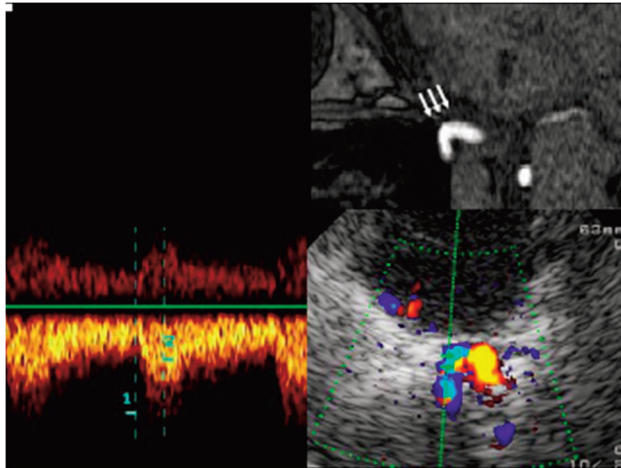


Fig 5. Assessment of the carotid siphon by using a transtemporal axial approach. Top: Time of flight MRA, axial source image, rotated 90° to correspond with the sonographic imaging plane, C3–4 segments (arrows). Bottom: TCCS, transtemporal approach, axial upper pontine plane. Right: Color-mode image demonstrating the C-shaped part of the carotid siphon. Left: Corresponding Doppler spectrum. Reprinted from Valdueza et al⁶ with permission from Thieme Medical Publishers, Stuttgart, Germany.

The shape was estimated on the basis of the sonographic findings. The part of the sphenoid bone that arises from the carotid furrow to the sella turcica serves as a readily identifiable anatomic landmark for this segment (Fig 5).

Finally, the C1–2 segment was examined in the coronal axis (anterior coronal plane), which required a 90° rotation of the sonographic probe again. These segments form the rising cisternal part and show a course from medial to lateral directions (Fig 6).

Results

Patient Characteristics

After screening for a sufficient temporal acoustic window (as previously defined) during a routine transcranial sonographic examination, we included 60 patients (32 men, 28 women) between 18 and 62 years of age (mean, 39 ± 11 years). Each subject underwent a bilateral examination.

Sonography Findings

The detection rates of all intracranial ICA segments were complete—with the exception of the C6 segment, which could not be displayed in 5 of 120 investigated segments. This segment was not displayed bilaterally in 1 male subject and on 1 side only in 3 female subjects. The subjects with undetectable C6 segments ranged from 32 to 45 years of age (range, 39 ± 5.7 years); in comparison, subjects with detectable C6 segments ranged from 18 to 62 years of age (range, 39 ± 11.2 years). In 58 vessels (48.3%), the course of the segment and the visible length (≥15 mm) allowed angle-corrected flow-velocity measurements. The peak-systolic flow/end-diastolic/mean-flow velocities were 66 ± 15/31 ± 8/43.6 ± 10.8 cm/s, with angle correction and 53 ± 14/25 ± 7/34.3 ± 8.8 cm/s without. C5 flow velocities were not measured because of an unfavorable insonation angle, as previously mentioned. The carotid siphon (C3–4) showed a straight course in 37% of subjects, a curved course in 62%, and a sigmoid course in 1%. Because of the contorted shape of this segment, angle-corrected flow velocities were not reliable. Instead, we measured the non-angle-

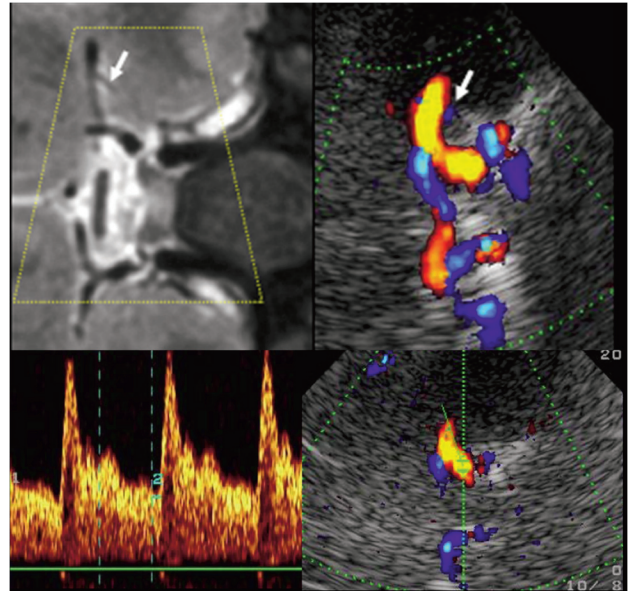


Fig 6. Assessment of the terminal (C1–2) segments of the ICA, by using a transtemporal coronal approach. Top left: MR imaging, T2-weighted image, coronal plane, rotated 90° counter-clockwise. Flow voids in the C5 ICA, C1–2 ICA, M1 MCA, and A1 ACA segments of both sides. Top right: TCCS, transtemporal approach, anterior coronal plane. Corresponding color-mode image demonstrates blood flow in the distal C1–2 ICA segment, partly in the carotid siphon, in the A1 ACA segment, and in the proximal M1 MCA segment bilaterally. Note the red and blue color codes, indicating flow directions toward and away from the transducer. Bottom: Corresponding color-mode and Doppler spectrum of the C1–2 ICA segment. Reprinted from Valdueza et al⁶ with permission from Thieme Medical Publishers, Stuttgart, Germany.

corrected maximal flow in this segment, realizing the limited value of the results. The peak-systolic flow/end-diastolic/mean-flow velocities were 57 ± 17/25 ± 8/36.1 ± 10.5 cm/s.

The terminal ICA (C1–2) was displayed in all cases. The course and visible length of the segment was ≥15 mm in 9 of 120 (7.5%) subjects, allowing reliable angle-corrected flow measurements of this small subgroup only. Peak-systolic/end-diastolic/mean-flow velocities of the C1–2 segment were 93 ± 18/43 ± 6/75.9 ± 9.8 cm/s with angle correction and 77 ± 21/34 ± 10/48.7 ± 13.4 cm/s without.

For detailed results of mean values with an SD of peak-systolic flow and end-diastolic flow, PI and RI, and the vessel length, see the Table.

Discussion

This study shows that TCCS by using the transtemporal bone window is a good tool to evaluate the distal petrosal part and all intracranial segments of the ICA. Previous systematic evaluations of the intracranial parts of the ICA by TCCS by using a transtemporal approach restricted their systematic evaluation of the ICA to the coronal axis.^{5,6} Alternatively, we also used the axial insonation plane for examination of the intracranial ICA in our neurovascular laboratories. The axial plane allows the examination of parts of the ICA with a primarily horizontal course. This applied not only to the carotid siphon (C3–4 segments of the ICA) but also to the distal part of the petrosal ICA, which runs horizontally. We have termed the segment preceding C5 in this part of the ICA as the “C6 segment.”

Adding the axial insonation plane can overcome the limitation of the coronal transtemporal plane in examining the C6

Flow velocities of the intracranial ICA segments in subjects without cerebrovascular disease using the transtemporal approach

ICA Segment	Psyst (cm/s)	E-D (cm/s)	Mean (cm/s)	PI*	RI*	Length (mm)	Identified No. (%)
C6							
No AC	53 ± 14 (27–106)	25 ± 7 (13–48)	34.3 ± 8.8 (17.7–68.0)	0.83 ± 0.16 (0.49–1.32)	0.53 ± 0.07 (0.37–0.70)	15 ± 4 (5–26)	115 (96.7)
AC (33 ± 10°)	66 ± 15 (34–113)	31 ± 8 (17–52)	42.5 ± 10.0 (26.0–72.3)	0.83 ± 0.17 (0.46–1.32)	0.53 ± 0.07 (0.35–0.70)	18 ± 2 (15–26)	58 (48.3)
C3–4							
No AC	57 ± 17 (31–105)	25 ± 8 (12–53)	36.1 ± 10.5 (18.3–68.7)	0.89 ± 0.17 (0.56–1.44)	0.55 ± 0.06 (0.41–0.70)	n.d.	120 (100)
C1–2							
No AC	77 ± 21 (33–140)	34 ± 10 (12–65)	48.7 ± 13.4 (19.0–90.0)	0.89 ± 0.16 (0.59–1.40)	0.55 ± 0.06 (0.42–0.72)	11 ± 2 (5–21)	120 (100)
AC (37 ± 10°)	93 ± 18 (64–118)	43 ± 6 (34–49)	59.9 ± 9.8 (44.0–71.3)	0.82 ± 0.13 (0.62–1.0)	0.53 ± 0.05 (0.44–0.61)	16 ± 2 (15–21)	9 (7.5)

Note:—Psyst indicates peak-systolic flow velocity; E-D, end-diastolic flow velocity; Mean, mean-flow velocity; ICA, internal carotid artery; PI, pulsatility index; RI, resistance index with standard deviation and range (in parentheses); ICA C6, distal petrosal part of the ICA; ICA C3–4, carotid siphon; ICA C1–2, distal part of the siphon and terminal segment of the ICA. AC, angle-corrected measurement, with the mean angle in parentheses; No AC, no angle correction; angle-corrected flow-velocity measurements were obtained if the vessel segment was visible for at least 15 mm; n.d., not done.

* With standard deviation and range (in parentheses).

and C3–4 segments of the intracranial ICA. However, because of its curved or contorted course, which results in an unfavorable insonation angle, the flow-velocity measurements of the C3–4 segments will provide only unreliable results. This finding is also true for the transtemporal coronal plane or the transorbital approach. For this reason, we reported the results collected without angle correction. Angle correction for the C1–2 segments was applicable for only a small subgroup because the visible length of the segment fell under the value of 15 mm for reliable angle-corrected flow measurement in most cases. Insonation was, however, more favorable for the C3–4 segments, which makes the non-angle-corrected flow velocities reliable. Failed detection of the C6 segment in 5 of 120 examined vessels—despite the presence of an excellent temporal acoustic bone window—may be related to the thickness of the osseous layer on the horizontal part of this vessel. Jurgita et al⁵ and Valaikiene et al,⁶ by using the coronal approach, also included the distal petrosal part (the part of the ICA that we referred to as the C6 segment) in their measurement of the C5 segment. This difference should be considered when comparing the TCCS screen shots shown in their publications with our findings. Because of the nearly 90° insonation angle, we regarded the TCCS measurements of the C5 segment (only examinable in the coronal plane) as unreliable. Consequently, we did not perform flow measurements of this segment.

Intracranial atherosclerosis is found in approximately 5%–10% of patients with stroke.^{10,11} The ICA has been reported as the most frequent site of intracranial stenosis, accounting for approximately 50% of cases.¹² Digital subtraction angiography remains the gold standard for detecting intracranial ICA stenoses; however, because of its invasive character, MR angiography (MRA) is frequently used instead. One drawback associated with MRA is its susceptibility to artifacts, especially in the contorted parts of the intracranial ICA, caused by flow-void phenomena. This problem can be overcome (at least partly) only by using contrast-enhancing agents.¹³

TCCS enables the examiner to discriminate all segments of the intracranial ICA and is a fast and inexpensive method of screening patients with suspected ICA stenosis. A limiting factor is a missing transtemporal acoustic window. The frequency of insufficient transtemporal acoustic windows in this

study was 14%, which is in the range that other examiners reported (approximately 11% in typical stroke populations).¹⁴ A skilled examiner is also required to avoid operator-dependent results.

The restriction to subjects with a sufficient acoustic temporal bone window is 1 limitation of this study; however, the idea behind this study was to determine normal values of flow velocities and the visible length of the ICA segments. When creating reference values for stenosis of the intracranial ICA,⁶ one should keep in mind that partly unfavorable insonation angles will limit validity. This was true in this study, especially for the C1–2 segments, which revealed a minimum visible length ≥15 mm as a prerequisite for angle correction in only 9 of 120 vessels. Indirect criteria like turbulence, segmental flow increase, musical murmur, or a change in the Doppler flow spectrum (eg, flattened systolic-flow acceleration) may be more reliable. With the expanding potential of intravascular stent placement of the intracranial vessels, including the ICA,^{15,16} TCCS may be an important screening and follow-up tool in patients with cerebrovascular disease that involves the intracranial part of the ICA. Furthermore, an analysis of the proximal parts of the intracranial ICA may also be helpful in examining the hemodynamic consequences of extracranial high-grade ICA stenosis, thus allowing a better graduation of stenoses. Finally, the coronal transtemporal approach may be helpful in differentiating a terminal ICA stenosis from proximal MCA pathology.

Conclusions

TCCS by using the transtemporal approach is a sufficient method for examining all intracranial parts of the ICA. With the expanding potential of endovascular treatment, this technique may serve as an important screening and follow-up tool in patients with vascular pathology.

References

- Seidel G, Kaps M, Gerriets T. **Potential and limitations of transcranial color-coded sonography in stroke patients.** *Stroke* 1995;26:2061–66
- Gerriets T, Postert T, Goertler M, et al. **DIAS I: duplex-sonographic assessment of the cerebrovascular status in acute stroke—a useful tool for future stroke trials.** *Stroke* 2000;31:2342–45

3. Gerriets T, Goertler M, Stolz E, et al. **Feasibility and validity of transcranial duplex sonography for diagnosis in patients with acute stroke.** *J Neurol Neurosurg Psychiatry* 2002;72:17–20
4. Hu HH, Luo CL, Sheng WY, et al. **Transorbital color Doppler flow imaging of the carotid siphon and major arteries at the base of the brain.** *AJNR Am J Neuroradiol* 1995;16:591–98
5. Jurgita V, Felix S, Thilo H, et al. **Transcranial color-coded duplex sonography of the carotid siphon: the coronal plane approach.** *Clin Imaging* 2002;26:81–85
6. Valaikiene J, Schuierer G, Ziemus B, et al. **Transcranial color-coded duplex sonography for detection of distal internal carotid artery stenosis.** *AJNR Am J Neuroradiol* 2008;29:347–53
7. Giller CA. **Is angle correction correct?** *J Neuroimaging* 1994;4:51–52
8. Valdueza JM, Schreiber SJ, Röhl J, et al. *Neurosonology and Neuroimaging of Stroke.* Stuttgart, Germany: Thieme Medical Publishers; 2008:25–28
9. Huber P. *Cerebral Angiography.* 2nd ed. Stuttgart, Germany: Thieme Medical Publishers; 1982
10. Caplan LR, Gorelick PB, Hier DB. **Race, sex, and occlusive cerebrovascular disease: a review.** *Stroke* 1986;17:648–55
11. Sacco RL, Kargman DE, Gu Q, et al. **Race-ethnicity and determinants of intracranial atherosclerotic cerebral infarction: The Northern Manhattan Stroke Study.** *Stroke* 1995;26:14–20
12. Akins PT, Pilgram TK, Cross DT 3rd, et al. **Natural history of stenosis from intracranial atherosclerosis by serial angiography.** *Stroke* 1998;29:433–38
13. Jung HW, Chang KH, Choi DS, et al. **Contrast-enhanced MR angiography for the diagnosis of intracranial vascular disease: optimal dose of gadopentetate dimeglumine.** *AJR Am J Roentgenol* 1995;165:1251–55
14. Krejza J, Swiat M, Pawlak MA, et al. **Suitability of temporal bone acoustic window: conventional TCD versus transcranial color-coded duplex sonography.** *J Neuroimaging* 2007;17:311–14
15. Bose A, Hartmann M, Henkes H, et al. **A novel, self-expanding, nitinol stent in medically refractory intracranial atherosclerotic stenoses: the Wingspan study.** *Stroke* 2007;38:1531–37. Epub 2007 Mar 29
16. Fiorella D, Levy EI, Turk AS, et al. **US multicenter experience with the Wingspan stent system for the treatment of intracranial atheromatous disease: periprocedural results.** *Stroke* 2007;38:881–87
17. Schünke M, Schulte E, Schumacher U. *Prometheus Lernatlas der Anatomie: Kopf und Neuroanatomie.* Stuttgart, Germany: Thieme Medical Publishers; 2006
18. Osborn AG. *Diagnostic Cerebral Angiography.* 2nd ed. Philadelphia: Lippincott Williams & Wilkins; 1999